



The MitoLuc Assay System for Accurate Real-Time Monitoring of Mitochondrial Protein Import Within Mammalian Cells

Hope I. Needs, James S. Lorriman, Gonçalo C. Pereira[†] Jeremy M. Henley and Ian Collinson^{*}

School of Biochemistry, University of Bristol, Bristol BS8 1TD, UK

Correspondence to Ian Collinson: ian.collinson@bristol.ac.uk (I. Collinson) @hopeneeds (H.I. Needs), @JamesLorriman (J.S. Lorriman), @MitoPereira_GC (G.C. Pereira), @IanofBristol_GC, @LabCollinson (I. Collinson)

<https://doi.org/10.1016/j.jmb.2023.168129>

Edited by William Clemons

Abstract

Mitochondrial protein import is critical for organelle biogenesis, bioenergetic function, and health. The mechanism of which is poorly understood, particularly of the mammalian system. To address this problem we have established an assay to quantitatively monitor mitochondrial import inside mammalian cells. The reporter is based on a split luciferase, whereby the large fragment is segregated in the mitochondrial matrix and the small complementary fragment is fused to the C-terminus of a purified recombinant precursor protein destined for import. Following import the complementary fragments combine to form an active luciferase—providing a sensitive, accurate and continuous measure of protein import. This advance allows detailed mechanistic examination of the transport process in live cells, including the analysis of import breakdown associated with disease, and high-throughput drug screening. Furthermore, the set-up has the potential to be adapted for the analysis of alternative protein transport systems within different cell types, and multicellular model organisms.

© 2023 The Author(s). Published by Elsevier Ltd. This is an open access article under the CC BY license (<http://creativecommons.org/licenses/by/4.0/>).

Introduction

Since most proteins required for mitochondrial function are encoded in the nucleus and synthesised by cytoplasmic ribosomes, efficient targeting and translocation of proteins into mitochondria is critical.^{1,2} In recent years, impaired mitochondrial protein import has been implicated in a range of pathologies, including myopathies and neurodegeneration.^{3–7} Therefore, an understanding of the molecular basis for these processes, and how they break down, will be crucial for our understanding and alleviation of associated disease.

Until recently, monitoring protein translocation has only been possible by carrying out end-point time course assays *in vitro* in isolated mitochondria,

wherein import is detected by radioactivity and Western blotting-based outputs.^{8–10} These classical assays have been crucial for seminal studies of our understanding of protein translocation in mitochondria (and bacteria); however, they are laborious and time consuming, and the resultant data are noisy, discontinuous, and not amenable to kinetic analysis and modelling. Moreover, the poor time resolution means that the initial fast phase of the reaction cannot be observed. Another caveat is that the results generated *in vitro* are not necessarily representative of what is happening within the whole cell. Therefore, new approaches are required to describe the individual steps that make up import and to understand the process *in vivo*.

Several alternative methods to achieve real-time monitoring of protein interactions and trafficking

have been described over the past couple of decades, but all have significant limitations, as discussed previously.^{11,12} Split-fluorophore systems¹³ are reliant on slow chromophore maturation (slower than the import reaction), which obscures the kinetics of the reaction of interest. Similarly, β -galactosidase assays have been used to monitor protein translocation through the nuclear envelope and plasma membrane,¹⁴ and could in theory be applied to mitochondria. However, these assays rely on reporter oligomerisation and product accumulation, hindering its ability to monitor import kinetics. Technology such as SNAP-tags can improve the time resolution of standard Western blotting-based import assays,¹⁵ but these are still laborious and cannot generate continuous import data. Thus, there has been a real need for innovative rapid and efficient experimental systems for real-time monitoring of mitochondrial protein import into isolated mitochondria, as well as within live cultured cell systems and *in vivo* within living multicellular model organisms.

NanoLuc Binary Technology (NanoBiT) is a highly sensitive, specific, and stable bioluminescence-based reporter system that utilises a small luciferase subunit derived from a deep-sea shrimp.¹⁶ This technology was originally developed by Promega¹¹ to monitor protein–protein interactions within living cells. It is a split luciferase, complementation-based system that relies on the binding of 11S (also known as LgBiT), an 18 kDa fragment of NanoLuc, and pep114 (also known as SmBiT), a small, 1.3 kDa peptide of 11 amino acids, which is the final β -strand of NanoLuc.¹¹ The resulting fully functional NanoLuc enzyme can convert furimazine to furimamide, producing a bioluminescent signal that can be detected with a luminometer.^{11,17} Pep86 (also known as HiBiT) is a high-affinity variant of pep114 (Kd 0.7 nM *versus* 190 μ M, respectively), also developed by Promega.¹¹

Recently, we have adapted and optimised this technology to monitor protein transport across biological membranes.¹² In essence, the 11S fragment is contained within a reconstituted or native vesicle/ organelle/ cell and the small fragment (*e.g.*, pep86) is fused to the protein destined for transport—*e.g.*, at the C-terminus of a bacterial pre-secretory protein or mitochondrial precursor (Figure 1(A)). Protein translocation is then monitored as the pep86-tagged protein crosses the membrane and associates with the encapsulated 11S. Under the conditions deployed, the binding of the two fragments to form the active luciferase is an order of magnitude faster than protein transport.¹² Thus, the luciferase signal reports faithfully on the detailed time-resolved kinetics of import, rather than the maturation of the luciferase.^{12,18} Importantly, it reduces the timescale of data acquisition from days (for classical assays involving radioactivity and/ or Western blotting) to minutes.

Its application to the analysis of protein translocation for bacterial secretion has been instrumental in the elucidation of the underlying molecular mechanism for transport.^{19,20}

We first demonstrated the utility of this new system by monitoring protein import into mitochondria isolated from yeast,¹² which we now call MitoLuc. In this case, 11S is constrained within the matrix for association with imported pep86 at the C-terminus of the precursor (precursor-pep86; Figure 1(A)). The nuts-and-bolts of the mitochondrial assay have been previously validated for the yeast system, demonstrating that luminescence is indeed a *bona fide* measure of protein import. Importantly, we have shown that increasing concentrations of precursor correlate linearly with the signal, until the import sites become saturated,¹⁸ so we know we are observing import.

The data generated is of sufficient quality to enable mathematical modelling approaches to help define the kinetic parameters underlying mitochondrial protein import.¹⁸ Using this MitoLuc system we investigated how two major driving forces, $\Delta\psi$ and ATP hydrolysis, contribute to import through the TIM23^{MOTOR} complex, and how the process is affected by specific properties of the precursor protein.¹⁸ These analyses could not have been achieved previously, particularly as the endpoint (amplitude) alone—the total amount of imported material of the assay, reported by the classic assay, is insufficient to understand the mechanism. Measuring both the amplitude and the rates by MitoLuc led to a basic model for import, revealing a surprising and fundamental feature, whereby the reaction proceeds in two distinct steps: one at the outer membrane (TOM) and the other at the inner (TIM23).

While the new *in vitro* assay has proved insightful, it does have its limitations; particularly in view of the analysis of mitochondria in isolation. First of all, it appears that the recuperative powers of isolated mitochondria are insufficient to maintain the $\Delta\psi$ to drive multiple rounds of import through each translocation site.¹⁸ Secondly, the interplay of the import machinery with regulatory cytosolic factors are all lost when studying purified mitochondria. This motivated us to adapt the assay to monitor import within intact cells. Such an assay would have the added advantage of observing fully fit mitochondria in their native state within the cytosol, that have not been subject to the physical trauma associated with isolation.

The assay we developed followed the principles devised for isolated yeast mitochondria (Figure 1(A)),¹² but utilising permeabilised live mammalian cells (Figure 1(B)). This *in cellular* (in-cell) version of the import assay provides accurate data with a high signal-to-noise ratio, comparable to the traces collected from isolated mitochondria, with the added bonus of context—*i.e.*, the ability to relate import activity and failure to the biology of the cell.

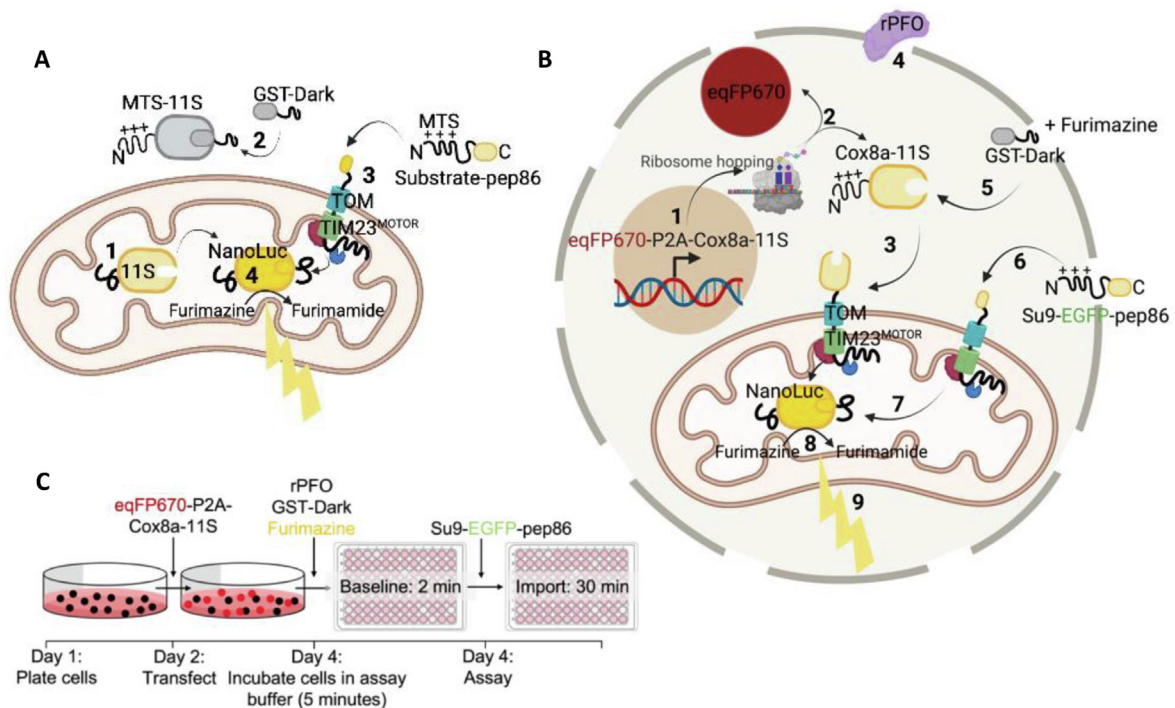


Figure 1. The MitoLuc Assay System for Monitoring Mitochondrial Protein Import in Yeast Mitochondria and Permeabilised Cells. (A) Schematic showing concept of the MitoLuc system to monitor mitochondrial import in isolated yeast mitochondria. Mitochondria were isolated from yeast producing a fusion of the mitochondrial targeting presequence (MTS) and the large fragment of split MitoLuc, 11S (MTS-11S). The resultant preparation with matrix localised 11S (with cleaved MTS) was deployed in the import assay: (1). GST-Dark is added to bind non-mitochondrial 11S, decreasing background signal (2). A pep86-tagged substrate protein (containing an N-terminal MTS; Su9-EGFP-pep86) is added and targeted to the mitochondrial matrix (3). The MTS is cleaved and pep86 binds to 11S in the matrix, forming MitoLuc (4). This converts furimazine to furimamide producing a luminescent signal. Schematic created using BioRender. **(B)** Schematic showing the concept of the permeabilised MitoLuc import assay system in live mammalian cells. DNA encoding eqFP670 (far red fluorophore) followed by a P2A region and Cox8a-11S is transcribed in the nucleus and translated in the cytosol (1), leading to the production of cytosolic eqFP670 and mitochondrially targeted Cox8a-11S (2). Cox8a-11S is translocated to the mitochondrial matrix *via* the presequence pathway (3). At the time of the assay, MitoLuc assay buffer containing 3 nM rPFO is added, which perforates the plasma membrane (4) whilst retaining intact mitochondria. This allows other substrates, drugs, furimazine, and proteins to enter the cells. One such protein is GST-Dark, which mops up any remaining cytosolic 11S (5), preventing background signal from cytosolic binding. Following a baseline read, a pep86 containing precursor is added (in this case Su9-EGFP-pep86; (6)) which is translocated into mitochondria where it binds to 11S (7), forming the functional MitoLuc enzyme, which converts furimazine to furimamide (8), producing a bioluminescent signal corresponding to import (9). Schematic created using BioRender. **(C)** Experimental outline of the permeabilised MitoLuc assay. On day 1, cells are plated, and are subsequently transfected with eqFP670-P2A-Cox8a-11S DNA on day 2. On day 4, the day of the assay, media is replaced with assay buffer containing furimazine, rPFO, and GST-Dark and incubated for 5 minutes prior to carrying out a 2 minute baseline read, followed by injection of the Su9-EGFP-pep86 protein and a 30-minute kinetic import read for luminescence corresponding to protein import.

The new in cell assay is outlined in [Figure 1\(B\)](#) with a full experimental outline in [Figure 1\(C\)](#).

Results

Assay outline

Cells are first transfected with DNA encoding eqFP670 (far red fluorophore) followed by a P2A region and Cox8a-11S. This is transcribed in the nucleus and translated in the cytosol, leading to

the production of cytosolic eqFP670 and mitochondrially targeted Cox8a-11S. Cox8a-11S is translocated to the mitochondrial matrix *via* the presequence pathway. At the time of the assay, import buffer containing 3 nM rPFO is added, which perforates the plasma membrane whilst retaining intact mitochondria. This allows other substrates, drugs, furimazine, and proteins to enter the cells. At this point, GST-dark is added, which binds any remaining cytosolic 11S, preventing background signal from cytosolic

binding. Following a baseline read, a pep86 containing precursor is added, which is translocated into mitochondria where it binds to 11S, forming the functional MitoLuc enzyme, which converts furimazine to furimamide, producing a bioluminescent signal corresponding to import *via* the presequence pathway (Figure 1 (B) and (C)).

Characterisation and optimisation of assay components

To quantify expression levels of mitochondrial 11S, which without the complementing peptide is colourless, a P2A bicistronic system was established to drive the stoichiometric production of the fluorescent protein eqFP670.²¹ This enabled the verification, quantification and normalisation of 11S expression, by virtue of the fluorescent co-expressed reporter: importantly, eqFP670 near-infrared excitation ($\text{Ex}_{\text{eqFP670}}$ 605 nm)²² is far enough away from 11S luminescence (405 nm)¹¹ to keep interference to a minimum.

Traditionally, cell permeabilisation for assessing mitochondrial physiology is accomplished using mild detergents such as digitonin or saponin. However, they are also known to permeabilise the mitochondrial outer membrane. Whilst this prospect is tolerable for assessing respiratory function, it is far from ideal for the analysis of protein import. So instead, we deployed recombinant perfringolysin (rPFO): a cholesterol-dependent, selective cytolysin,²³ which has negligible mitochondrial side-effects up to 10 nM.²⁴ Upon oligomerisation, rPFO forms pores in the plasma membrane, allowing solutes and proteins of up to 200 kDa to rapidly equilibrate between the cytoplasm and extracellular medium.^{25,26}

When cells are challenged with 5 mM succinate and 1 mM ADP, there is no respiratory response (change in oxygen uptake); this is expected, because they fail to permeate the plasma membrane (Figure 2(A)). However, upon addition of 3 nM rPFO the rate of oxygen consumption increases rapidly (Figure 2(A)), as succinate and ADP flood the cytosol and enter mitochondria through respective metabolite carrier proteins. Thus, demonstrating effective plasma membrane permeabilisation. The short delay prior to the burst of oxygen consumption is most likely due to the time taken for pore assembly. Importantly, the addition of exogenous cytochrome *c* during ADP-sustained respiration resulted in only a small change, indicating that the outer membrane was largely intact and had retained endogenous cytochrome *c*. The minor change elicited by the addition of cytochrome *c* nicely shows that exogenous proteins rapidly gain access to the mitochondrial surface. Therefore, rPFO treatment effectively permeabilises the plasma membrane to metabolites and proteins without compromising mitochondrial integrity or respiratory function.

A major issue with the MitoLuc import assay is the background signal arising from unimported 11S in the cytosol, release of internalised 11S, or its presence in the external media resulting from lysed cells. To mitigate the background signal, we included an inactivated pep86 peptide fused to GST that can access extra-mitochondrial 11S, but not the matrix encapsulated reservoir.¹² A single amino acid substitution of a critical catalytic arginine residue of pep86 creates DarkBiT, which, upon binding to 11S, prevents catalysis by the formed NanoBiT complex.^{12,27} Thus, glutathione S-transferase fused to the DarkBiT peptide (GST-DarkBiT, also known as GST-Dark) quenches off-target luminescence arising from outside the matrix (Figure 1(A) and (B)). This mopping-up of external (in this case cytosolic) 11S has proved to be very effective in all other systems tested so far, including the assay developed for monitoring import into yeast mitochondria.¹⁸

Addition of purified GST-Dark to a final concentration of 20 μM (20-fold higher than precursor-pep86 fusion) considerably reduced the luminescence signal (Figure 2(B) and (C)), which we attribute to binding and inactivation of residual 11S in the cytosol or external medium. This also prevents the non-mitochondrial 11S from sequestering precursor-pep86 *en route* to the mitochondria, and thereby ensuring the luminescent signal is solely produced by the formation of MitoLuc in the matrix.^{12,18} This quenching step is critical as evidently ~60% of the luminescence signal arises from non-matrix sources (Figure 2(B) and (C)). Importantly, the remaining (matrix) signal is characteristic of import kinetic profiles seen with isolated mitochondria (Figure 2(B), red trace).¹⁸

At the same time as rPFO and GST-Dark addition to cells, the furimazine stock solution was added at a dilution of 1:800, as determined by a titration experiment to define the optimal dilution (Figure 2 (D) and (E); slopes with error are shown in supplementary Figure S1). At lower dilutions (higher concentrations) of furimazine (1:50 and 1:100), furimazine has an inhibitory effect on mitochondrial import, probably due to respiratory toxicity, consistent with previous data in yeast mitochondria.¹²

The in-cell MitoLuc assay requires ATP and PMF

As an import substrate, the engineered precursor protein Su9-EGFP-6xHis-pep86 was cloned for recombinant expression and purified in urea in an unfolded state. This protein contains the potent MTS of fungal Su9 for targeting to the mitochondrial matrix, as well as an EGFP fluorescent reporter. To characterise the specificity of the assay system for import *via* the presequence (TIM23^{MOTOR}) pathway into the matrix, cells were treated with 1 μM antimycin A

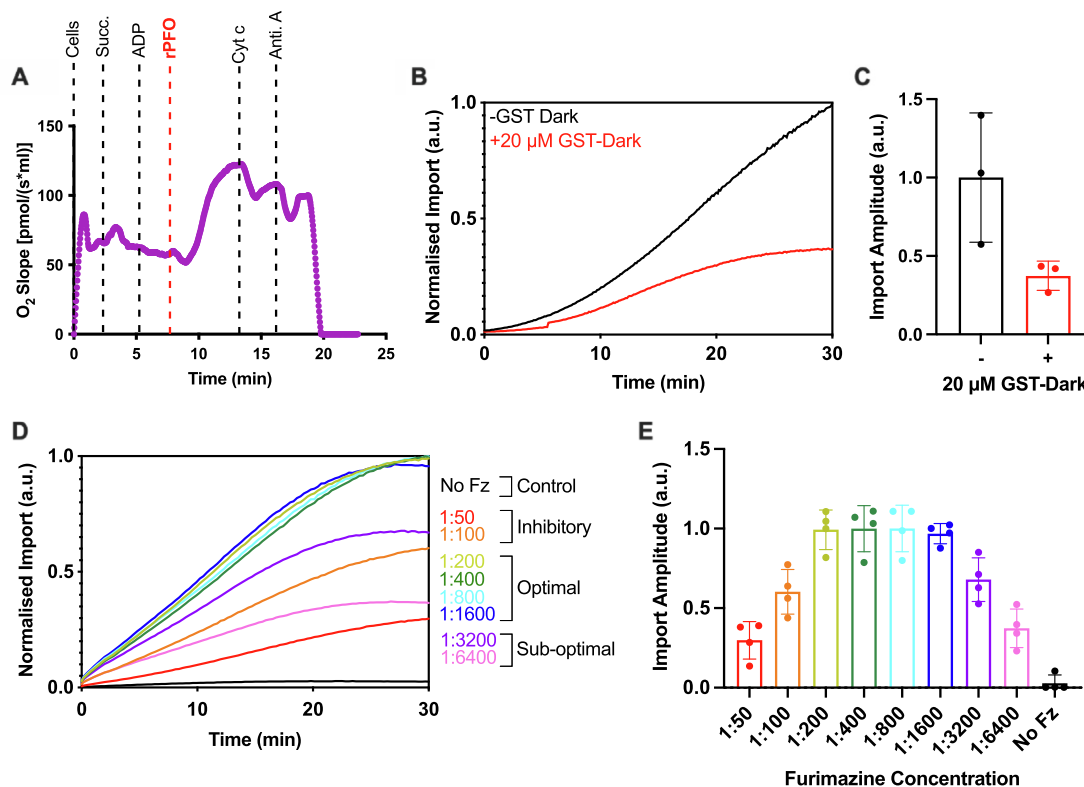


Figure 2. Permeabilised Cell MitoLuc Assay System Optimisation: rPFO, GST-Dark, and Furimazine. (A) Oroboros oxygraph trace showing mitochondrial respiration in HeLa cells and the response to various stimuli/poisons. Cells are stimulated by addition of 5 mM succinate (Succ.) and 1 mM ADP prior to addition of 3 nM rPFO, which allows the substrates to access mitochondria. Cytochrome *c* (Cyt *c*; 10 μ M) and antimycin A (Anti. A; 1 μ M) are subsequently added, and the impact of these respiratory chain substrates on the oxygen consumption of the cells is measured. Representative trace shown. $N = 3$ biological repeats. (B) Average traces from the MitoLuc import assay in the absence (black) or presence (red) of 20 μ M GST-Dark, added to cells 5 minutes prior to the assay. Background was removed and data was normalised to cellular eqFP670 expression, and the maximum amplitude from the run, to allow comparison between runs regardless of raw values. $N = 3$ biological repeats, each with $n = 3$ technical replicates. (C) Maximum amplitude plotted from average import traces displayed in (B). Error bars display SD. (D) Average traces from the MitoLuc import assay showing import with a titration of furimazine (Fz; dilutions indicated as ratios of furimazine: assay buffer). Fz was applied to cells for 5 minutes prior to starting the assay, the MitoLuc assay was then carried out with a Su9-EGFP-pep86 precursor. Data was normalised as described in (B). $N = 4$ biological repeats, each with $n = 3$ technical replicates. (E) Maximum amplitude plotted from average import traces displayed in (D). Error bars display SD.

(A)—an inhibitor of complex III of the respiratory chain, and 5 μ M Oligomycin (O)—an inhibitor of the ATP synthase. Together, these drugs limit the capacity to maintain ATP and PMF, both of which are required for protein import: PMF to drive the transport of positive residues across the membrane and ATP for the mitochondrial Hsp70 ATPase (mtHsp70) of the matrix located motor domain of the TIM23^{MOTOR} complex.

The impact of the AO inhibitors on the respiratory function of the permeabilised cells was confirmed with a seahorse respirometer (Figure 3(A)). This corresponded to a $\sim 70\%$ reduction in the amplitude (total amount) of precursor import (Figure 3(B) and (C)). Interestingly, compromising the available ATP and PMF affects the shape of the import curve (Figure 3(B), red trace): a

reduction of a lag indicative of an impact also on the kinetics of the import reaction.¹⁸

The remaining $\sim 30\%$ of import activity, unaffected by AO, we assumed to be driven by residual PMF and ATP. Note that we could not use the more effective PMF-uncoupler CCCP because it interferes with the NanoLuc chemistry. To confirm this, we carried out imaging experiments to assess how the mitochondrial accumulation of TMRM (a proxy for membrane potential) is affected by AO treatment (supplementary Figure S2). This showed that the addition of AO depletes, but does not eliminate, the membrane potential; while the addition of CCCP abolishes it. These results are in line with the large reduction, but not complete inhibition, of import observed in the presence of AO (Figure 3

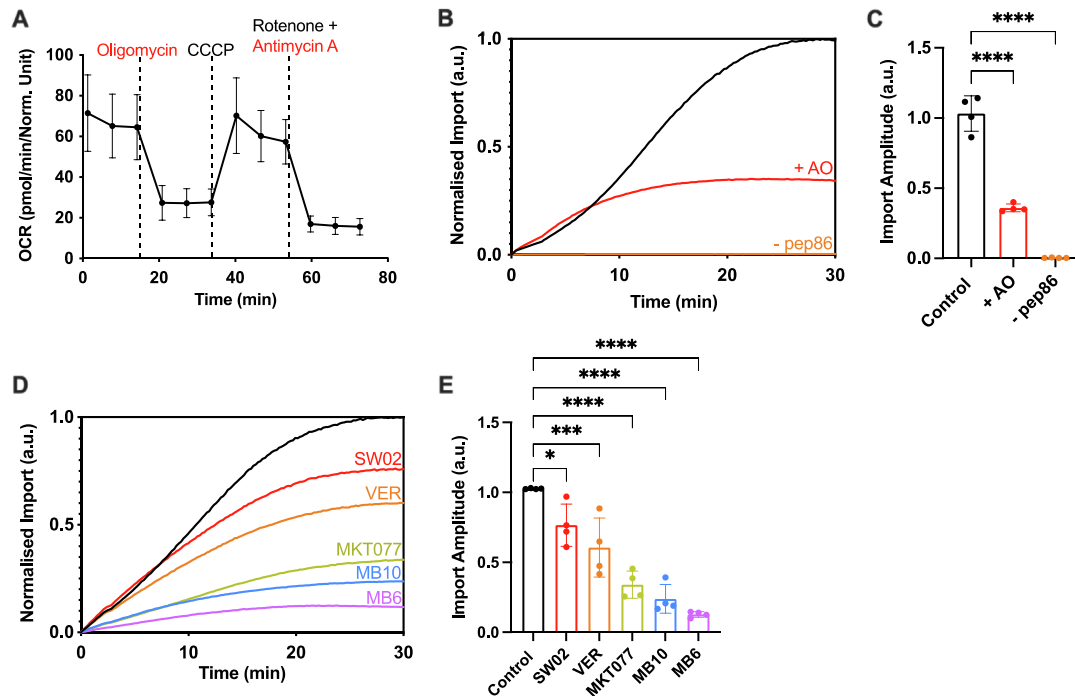


Figure 3. The Permeabilised MitoLuc Assay Monitors Import via the Presequence Pathway. (A) Mitochondrial stress test showing oxygen consumption rate (OCR) of cells when subjected to various respiratory chain substrates. HeLaGAL cells were grown for 48 hours prior to carrying out mitochondrial stress tests on a Seahorse XFe96. 1.5 μM oligomycin, 0.5 μM CCCP, 0.5 μM antimycin A, and 0.5 μM rotenone were added and their impact on mitochondrial oxygen consumption was measured. Data was normalised to cell density according to an SRB assay. $N = 6$ biological repeats, each with $n = 3$ technical replicates. (B) MitoLuc import trace for Su9-EGFP-pep86 in the absence (black) or presence (red) of PMF inhibitor AO (1 μM antimycin A, 5 μM oligomycin), or in the absence of pep86 containing precursor (orange). AO was applied to appropriate wells for 5 minutes prior to monitoring the import of the precursor (Su9-EGFP-pep86) using the MitoLuc assay. Resulting normalised average traces are shown. $N = 4$ biological repeats, each with $n = 3$ technical replicates. (C) Maximum amplitude plotted from average traces shown in (B). Error bars display SD. One-way ANOVA and Tukey's post hoc test were used. (D) MitoLuc import traces in the presence of small molecule inhibitors of the import machinery. No drug (black), SW02 (20 μM , red), VER (20 μM , orange), MKT077 (20 μM , green), MB10 (30 μM , blue), or MB6 (10 μM , purple) were applied to cells for 5 minutes prior to starting the assay, the MitoLuc assay was then used to monitor import of a purified precursor (Su9-EGFP-pep86). Resulting normalised average traces are shown. $N = 4$ biological repeats, each with $n = 3$ technical replicates. (E) Maximum amplitude plotted from average traces shown in (D). Error bars display SD. One-way ANOVA and Tukey's post hoc test were used to determine significance.

(B) and (C)). The dependence of both the kinetics and total yield of import on ATP and the PMF confirms that the luminescent signal is a true measure of the mitochondrial presequence import pathway.

The in-cell MitoLuc assay is applicable to both artificial and native precursor proteins

To ensure the assay is applicable to other more native proteins, we purified a recombinant ACP1-pep86 precursor protein and carried out import assays (supplementary Figure S3). The data showed that the assays yielded import traces with similar kinetics compared to the Su9-EGFP-pep86 protein. Therefore, as expected, the import apparatus is unhindered by the transport of

relatively stably folded proteins like the β -barrelled GFP.

The import kinetics determined by the in-cell MitoLuc assay mirror those acquired by the classical approach

To ensure our assay was reporting kinetics in line with the classical approach (e.g. Western blotting-based import assays), we investigated the accumulation of the mature (MTS-cleaved) version of our Su9-EGFP-pep86 protein in the mitochondria of HeLa cells over time (supplementary Figure S4).

HeLa cells were incubated in MitoLuc assay buffer containing rPFO, followed by addition of Su9-EGFP-pep86. Import was quenched by the

addition of the VOA (Valinomycin, Oligomycin, Antimycin A) cocktail at given time points. Mitochondria were then isolated from the cells, and Western blotting showed the relative abundance of the full-length and cleaved proteins at each time point. The ratio of accumulated cleaved (mature)/full-length protein is representative of protein import, as maturation occurs in the matrix. The data, as expected, is very noisy, but it is clear that the import kinetics roughly mirror the results of the MitoLuc assay (supplementary Figure S4). Note that the cleaved MTS measured at $t = 0$ most likely occurred during mitochondrial isolation, due to residual ATP and PMF, despite the inhibitor cocktail (see also above and supplementary Figure S2).

The in-cell MitoLuc assay is sensitive to small molecule import inhibitors

Finally, the specificity of the assay was interrogated further by treating cells with drugs known to target various components of the import machinery (Figure 3(D) and (E)). Cells were subject to an acute treatment by incubation of the drug 5 minutes prior to beginning the MitoLuc assays. Various small molecules were deployed which target the TIM23 presequence pathway: MB10, which inhibits mtHSP70 or TIM44¹⁰; VER-155008, MKT077 and SW02—all of which target the mtHSP70 ATPase^{28–30}, and also MB6, an inhibitor of the MIA pathway³¹ for protein targeting to the intermembrane space (IMS).³²

All drug treatments were observed to induce a reduction in the total amount of imported precursor (Figure 3(D) and (E)); unsurprisingly so, in the cases of VER-155008, MKT077, and MB10. Interestingly, SW02, which enhances the ATPase activity of mtHSP70,³⁰ increased the rate of import, but reduced the overall yield, suggestive of more subtle perturbation of the import process. The dramatic effect of MB6 on import efficiency was unexpected, considering that the imported substrate (Su9-EGFP-pep86) is not supposed to require the MIA pathway.

Whilst all the drugs have an impact on the amplitude, there are also variations in the rates and the shape and complexity of the curve. These are intriguing observations that warrant further investigation in the manner achieved for isolated yeast mitochondria.¹⁸ Overall, the general dependencies and specific sensitivities we observed are consistent with faithful and accurate reporting of mitochondrial import.

Discussion

We have developed, optimised, and road-tested an assay to monitor mitochondrial protein import in real-time with the capacity to obtain accurate kinetic data of events happening inside

mammalian cells. The permeabilised cell MitoLuc assay works in HeLa cells and could be readily adapted for alternative immortalised or primary cell culture systems. Characterisation of the HeLa based system confirmed that the luminescence signal is an authentic measure of import *via* the presequence (TIM23^{MOTOR}) pathway, due to its dependence on ATP and the PMF, and sensitivity to several specific and well characterised small molecule import inhibitors.

This system is based on the same concepts that we described for isolated yeast mitochondria,^{12,18} enabled by permeabilisation using rPFO for accessibility of the necessary reagents, mitochondrial energisation, visualisation and experimentation (*e.g.*, inhibition). Remarkably, the permeabilisation preserves mitochondrial respiratory capacity and, insofar as we can tell, has not significantly perturbed the system. Specifically, addition of cytochrome *c* showed that the mitochondrial outer membrane remained largely intact. Therefore, from the point of view of characterisation of protein import activity, regulation, and consequences of failure, the assay is robust and informative of mitochondrial physiology in the native cellular environment (compared to an artificial stabilising solution).

Importantly, the assay removes the need for mitochondrial isolation, and the inevitable physical damage this entails. Therefore, the MitoLuc assay has the capability to investigate import in an unperturbed state in fully functional mitochondria. Despite the clear advantages, we should also consider that freely diffusing cytosolic factors may be lost or diluted due to permeabilisation. So, it could be that some of the peripheral regulatory aspects of the import process may be impaired or lost, and not observable. Although, once identified, lost regulatory factors could of course always be maintained exogenously. Future work will provide interesting and informative evaluation of how import within cells compares to import into isolated mitochondria.

A key advance is that this new assay also provides opportunities to study the import process of mammalian mitochondria. Intact and functional mitochondria are challenging to isolate from cultured cells. So, avoiding this damaging step enables the analysis of a wide range of genetically malleable mammalian cells. This is an important advance, freeing research of the restrictions of the classical model systems—beyond simple eukaryotes (yeast) and genetically intractable mammalian models (*e.g.*, mitochondria isolated from cows and rats). Furthermore, this system has several benefits over classical import assays. As with the import assay into isolated mitochondria, the data acquisition time is reduced significantly from a matter of days to less than 30 minutes. Moreover, the assay can be run in a multiplate reader for rapid collection of large data sets at high time resolution. This high throughput

capability will also facilitate small molecule screening ventures seeking drugs that modulate the import apparatus.

The permeabilised cell MitoLuc assay system can provide insight into the kinetics of import, aided by its sensitivity, allowing the detection of very small changes across all stages of the process. Furthermore, the time resolution and quality of the data (low noise) enables mathematical fitting to kinetic models—as demonstrated for import into isolated yeast mitochondria¹⁸—for the dissection and characterisation of the different stages of import. Remarkably, the data presented here is of comparable quality, indicating it is now possible to do so in whole cell systems. Beyond this, we envisage that it will be possible to further develop this system to study the behaviour of particularly interesting import substrates—such as PINK1, the aberrant import of which has been linked to early onset Parkinson's disease.³³ Likewise, we are now able to investigate further if and how certain aggregation prone protein variants (*e.g.*, APP, Tau and Htt), associated with neurodegeneration, affect the import machinery—as is suspected. So, watch this space!

The system could also be adaptable to monitor alternative import pathways, *e.g.*, *via* TIM23^{SOFT} for lateral insertion into the IMM, MIA for IMS trafficking and the TIM22 complex for presequence independent transport of the carrier superfamily to the IMM. Incorporation of 11S in the IMS will also enrich our understanding of the various import routes, to visualise the transient entry of clients of the TIM23 or TIM22 complexes, as well as the endpoint after IMS entry *via* MIA. Once the various import pathways can be monitored, the inhibitors tested here will help dissect the critical stages of each process.

A further goal will be to develop the assay system to primary cell cultures, such as neurons, and potentially also multi-cellular organisms. Aside from the additional challenges associated with the manipulation and imaging of primary cultures and model organisms, there are no technical barriers for the wider implementation of this assay into more interesting real-life situations. In this respect, it would be interesting to explore how mitochondrial import activity is affected in various models of disease, particularly those implicated with dysfunctional import.

Materials & methods

Reagents

All chemicals were of the highest grade of purity commercially available and purchased from Sigma, UK, unless stated otherwise. Aqueous solutions were prepared in ultrapure water, while for non-aqueous solutions, ethanol or DMSO was used as solvent instead.

Generation of Constructs

Constructs were generated by standard cloning techniques. PCR reactions were carried out using Q5 High Fidelity Hot Start DNA Polymerase (New England Biolabs (NEB), UK), using 20 pmol primers and 200 pg template DNA, as per manufacturers' instructions. Restriction digest reactions were carried out using NEB restriction enzymes at 37 °C for 45–60 min. Ligation reactions were carried out using T4 DNA Ligase (NEB) overnight at 16 °C, using a ratio of 1:3 vector to insert (50 ng total). Transformation was carried out by incubation of 10% of total ligation mix/50 ng plasmid DNA construct in 50 µl competent *E. coli* cells (α -select, XL1-Blue, or BL21-DE3 cells were used, depending on application; all originally sourced from NEB and obtained from lab made stocks, stored at –80 °C) for 30 min on ice, followed by heat shock (45 sec, 42 °C), and a further 15 min on ice. Cells were recovered by incubating in LB media at 37 °C for 1 h and plated on LB-agar plates containing appropriate antibiotic. Plasmids were prepared by mini or maxi preps using commercially available kits (Qiagen, UK and Promega, UK, respectively) following manufacturers' instructions, and verified by DNA sequencing using Eurofins Genomics, UK.

Protein purification

Protein expression was carried out exactly as described previously.¹² Pre-cultures of transformed BL21 (DE3) bacteria were grown overnight at 37 °C in LB with appropriate antibiotic. Secondary cultures were inoculated at 1:100 from pre-cultures, in 1–8 L of 2X YT supplemented with appropriate antibiotic. Secondary cultures were grown until mid-log phase, then induced with 1 mM IPTG or 0.2% (w/v) Arabinose and grown for a further 3 h at 37 °C. Cells were harvested by centrifugation, resuspended in ice-cold TK buffer (20 mM Tris, 50 mM KCl, pH 8.0), cracked in a cell disruptor at 4 °C, and clarified by centrifugation at 38,000 rpm for 45 min at 4 °C.

GST tagged recombinant perfringolysin (rPFO). rPFO is a selective cytolysin,²³ used as a permeabilisation agent in permeabilised cell MitoLuc import assays. Supernatant (soluble fraction) was loaded onto a 5 ml GSTrap 4B column (GE Healthcare, UK) and the column was washed with TK buffer. The peptide was eluted using freshly prepared 10 µM reduced glutathione in TK buffer. Eluted fractions were pooled and loaded onto a 5 ml anionic exchanger (Q- column; GE Healthcare). A salt gradient of 0–1 M KCl was applied at 5 ml/min over 20 min. The eluted fractions containing the protein were confirmed by SDS-PAGE with Coomassie staining, then pooled and concentrated by centrifugation at 4000 xg in a 50,000 MWCO PES VivaSpin concentrator (Sartorius) at 4 °C. The final protein

concentration was determined by A280 (extinction coefficient: $117,120 \text{ M}^{-1} \text{ cm}^{-1}$). The protein was aliquoted, snap frozen, and stored at $-80 \text{ }^\circ\text{C}$. This protein was observed to have low stability once thawed, therefore a single aliquot was used per experiment.

GST-Dark peptide. GST-Dark is an inactive version of pep86 (DarkBiT;²⁷) fused to GST. It is used to quench any cytosolic 11S in import assays, preventing background signal from cytosolic binding of pep86 and 11S. GST-Dark was prepared as described previously.¹² Supernatant was loaded onto a GSTrap 4B column in TK buffer and purification was carried out exactly as for rPFO without the ion-exchange chromatography. Analysis, yield, and freezing was carried out exactly as for rPFO. For concentration, a 10,000 MWCO concentrator was used. Protein concentration was determined based on an extinction coefficient of $48,360 \text{ M}^{-1} \text{ cm}^{-1}$.

His tagged Su9-EGFP-pep86. Su9-EGFP-pep86 is a precursor protein with a Subunit 9 mitochondrial targeting pre-sequence (Su9-MTS) from *Neurospora crassa*, an EGFP reporter domain, and a pep86 peptide. Inclusion bodies (insoluble fraction) were solubilised in TK buffer supplemented with 6 M urea before loading onto a 5 ml HisTrap HP column (GE Healthcare). The column was first washed with TK + 6 M urea followed by TK + 6 M Urea + 50 mM imidazole. The protein was eluted in 300 mM imidazole. Eluted fractions containing the desired protein were pooled and loaded onto a 5 ml cationic exchanger (S- column; GE Healthcare). A salt gradient of 0–1 M KCl was applied over 20 min (at 5 ml/min) and the protein was eluted in 5 ml fractions. Salt was then removed by spin concentration, followed by dilution in TK buffer containing 6 M urea. Analysis, yield, and freezing were carried out exactly as for rPFO. For concentration, a 10,000 MWCO concentrator was used. Protein concentration was determined based on an extinction coefficient of $28,880 \text{ M}^{-1} \text{ cm}^{-1}$.

ACP1-pep86. ACP1-pep86 was used as an alternative, native precursor protein for MitoLuc import assays, and was purified as described previously.¹⁸ Inclusion bodies (insoluble fraction) were solubilised in TK buffer supplemented with 6 M urea before loading onto a 5 ml HisTrap FF column (GE Healthcare). The column was first washed with TK + 6 M urea followed by TK + 6 M Urea + 50 mM imidazole. The protein was eluted in 300 mM imidazole. Eluted fractions containing the desired protein were pooled and loaded onto a 5 ml anionic exchanger (Q- column; GE Healthcare). A salt gradient of 0–1 M KCl was applied over 20 min (at 5 ml/min) and the protein was eluted in 5 ml fractions. Salt was then removed by spin con-

centration, followed by dilution in TK buffer containing 6 M urea. Analysis, yield, and freezing were carried out exactly as for rPFO. For concentration, a 10,000 MWCO concentrator was used. Protein concentration was determined based on an extinction coefficient of $14,440 \text{ M}^{-1} \text{ cm}^{-1}$.

Cell culture

HEK293T (ECACC) and glucose-grown HeLa (HeLaGLU; ATCC) cells were maintained in Dulbecco's Modified Eagle's Medium (DMEM; Gibco, UK) supplemented with 10% (v/v) foetal bovine calf serum (FBS; Invitrogen, UK) and 1% (v/v) penicillin–streptomycin (P/S; Invitrogen). Where OXPPOS dependence was required, HeLa cells were cultured in galactose medium (HeLaGAL) consisting of DMEM without glucose (Gibco) supplemented with 10 mM galactose, 1 mM sodium pyruvate, 4 mM glutamine, 10% FBS and 1% P/S. Cells were cultured in galactose media for at least 3 weeks prior to experiments on HeLaGAL cells. Cells were maintained in T75 ventilated flasks in humidified incubators at $37 \text{ }^\circ\text{C}$ with 5% CO_2 .

Cell transduction by transfection

HeLa cells were seeded and grown up to 70–80% confluency. At this point cells were transfected with 0.5–2 μg of the desired DNA using Lipofectamine 3000 reagent (Thermo Fisher Scientific, UK) using a 1:3 DNA to lipofectamine ratio and following the manufacturers' protocol. Cells were then grown for a further 24–72 hours prior to experimental analysis.

MitoLuc import assay

Cells were seeded in 6-well plates (300,000 cells/well) and transfected with eqFP670-P2A-Cox8a-11S after 24 h. They were incubated for a further 48 h at $37 \text{ }^\circ\text{C}$. After 48 h of 11S transfection, cells were seeded on standard white flat-bottom 96-well plates at 30,000 cells/well and import assays performed 16 h afterwards. Then, cells were washed three times with 200 μl HBSS (calcium and magnesium free) and incubated in HBSS imaging buffer (1 X HBSS (Thermo), 5 mM D-(+)-glucose, 10 mM HEPES (Santa Cruz Biotechnology, Germany), 1 mM MgCl_2 , 1 mM CaCl_2 , pH 7.4). A fluorescence read was taken at 605/670 nm using monochromators with gain set to allow maximum sensitivity without saturation, using a BioTek Synergy Neo2 plate reader, for normalisation of results against eqFP670 expression. Buffer was then removed and cells were incubated in MitoLuc assay buffer (225 mM mannitol, 10 mM HEPES, 2.5 mM MgCl_2 , 40 mM KCl, 2.5 mM KH_2PO_4 , 0.5 mM EGTA, pH 7.4) supplemented with 5 mM succinate, 1 μM rotenone, 0.1 mg/ml creatine kinase, 5 mM

creatine phosphate, 1 mM ATP, 0.1% (v/v) Prionex, 3 nM rPFO (purified in house), 20 μ M GST-Dark (purified in house), and 1:800 furimazine (Nano-Glo[®] Luciferase Assay System; Promega). Drugs or inhibitors were added to individual wells as described in figure legends. A baseline read of 30 sec of background luminescent signal was taken prior to injection of purified substrate protein (Su9-EGFP-pep86 or ACP1-pep86) to 1 μ M final concentration, followed by a further bioluminescence read corresponding to import, lasting 30 min. Bioluminescence was read using a BioTek Synergy Neo2 plate reader (Agilent, UK) or a CLARIOstar Plus plate reader (BMG LabTech, UK) without emission filters with gain set to allow maximum sensitivity without saturation, and with acquisition time of 0.1 sec per well. Row mode was used, and reads were taken every 6 sec or less, with wells in triplicate.

Classical western blot based import assay

HeLa cells were plated in a 6-well plate and incubated at 37 °C until they reached approximately 100% confluency. On reaching confluency, media was removed, cells were washed once in HBSS (Invitrogen) and 1 ml MitoLuc assay buffer was added (supplemented with 0.1 mg/ml CK, 5 mM CP, 1 mM ATP, 3 nM rPFO, 5 mM succinate, 1 μ M rotenone). Purified Su9-EGFP-pep86 protein was added to a final concentration of 1 μ M and cells were incubated at 37 °C for 30 min with samples being taken at the following time points (min): 0, 5, 10, 15, 20, 30. Samples were treated as follows: 100 μ l VOA cocktail (1 μ M valinomycin, 20 μ M oligomycin, 8 μ M antimycin A) was added to quench further import and then the MitoLuc assay buffer was removed. Cells were detached with Trypsin-EDTA solution (0.05% trypsin, 0.02% EDTA, Invitrogen) which was then quenched by the addition of complete DMEM media. Cells were then clarified by centrifugation at 1,000 xg for 2 min, media was removed, and the pellet was washed in HBSS before being clarified by centrifugation once again. The resulting cell pellet was frozen at -20 °C overnight. The following day the pellets were thawed on ice and mitochondria were isolated using the Mitochondrial Isolation Kit for Cultured Cells (Abcam; ab110170). In the final step, mitochondria were isolated by centrifugation at 12,000 xg for 30 min and the mitochondrial pellet was subsequently resuspended in sample buffer (2X LDS + 50 mM DTT).

Samples were heated at 95 °C for 5 min before the total mitochondrial sample was loaded on a 4–12% Bis-Tris Plus 10-well Bolt gel (Invitrogen). Samples were separated at 200 V for 25 min and subsequently transferred onto nitrocellulose membranes with NuPage Transfer Buffer (Novex) supplemented with 20% ethanol, using a semi-dry transfer system (Invitrogen). Membranes were

subsequently blocked for 1 h at room temperature in TBS-T (20 mM Tris, 1.5 M NaCl, 0.1% Tween 20) with 5% milk before being incubated with anti-GFP (1:1000, Chromotek 3H9) overnight at 4 °C. Membranes were extensively washed in TBS-T prior to being probed with anti-rat secondary antibody (1:10,000, Sigma A5795) for 1 h at room temperature. Membranes were subsequently washed with TBS-T, incubated with SuperSignal West Dura Extended Duration Substrate (ThermoScientific) and developed using an Odyssey FC Imaging System (LI-COR). Subsequent analysis and quantification of the blot was performed using Image Studio Lite.

Mitochondrial respiration analysis

Oxygraph assay. Cells were grown to confluency in T75 flasks, then harvested with trypsin, pelleted, and washed once with HBSS (Ca²⁺- and Mg²⁺-free), and finally resuspended in mannitol respiration buffer (225 mM mannitol, 10 mM HEPES, 2.5 mM MgCl₂, 40 mM KCl, 2.5 mM KH₂PO₄, 0.5 mM EGTA, pH 7.4). Respiratory function assays were carried out in a Oxygraph-2k (Oroboros Instruments, Innsbruck, Austria) at 37 °C in a 2 ml closed chamber with 5 million cells per run. Drugs were added as indicated in figure legends and respiration rates were calculated as the average value over a 45 sec window in DatLab 5 (Oroboros Instruments) and are expressed in nmol O₂ / min /mg protein.

Seahorse assay: mitochondrial stress test. Cells were seeded in 6-well plates (300,000 cells/well). The day prior to the assay, cells were seeded at 10,000 cells/well in 96 well Seahorse XF cell culture plates (Agilent, UK). The sensor cartridges were hydrated overnight with tissue culture grade H₂O in a non-CO₂ incubator at 37 °C as per manufacturer's instructions. On the day of the assay, H₂O in the sensor plate was replaced with Seahorse XF Calibrant (Agilent) and cells were washed with HBSS and incubated in Seahorse media (Seahorse XF assay medium (Agilent), 1 mM pyruvate (Agilent), 2 mM glutamine (Agilent), 10 mM D-(+)-galactose). Both sensor and cell plates were incubated in a non-CO₂ incubator at 37 °C for 1 h prior to the assay. The sensor plate was loaded with oligomycin (15 μ M for 1.5 μ M final concentration in wells; injector A), CCCP (5 μ M for 0.5 μ M final; injector B) and antimycin A and rotenone (5 μ M/5 μ M for 0.5 μ M/0.5 μ M final; injector C). The sensor plate was calibrated in the machine prior to loading cells and running a mitochondrial stress test using a Seahorse XFe96 analyser (Agilent). Following assays, cells were washed and fixed in 1% acetic acid in methanol at -20 °C overnight for sulforhodamine B (SRB) assays, which were used for normalising data to protein content.

SRB assay

For analysis of cell density based on cellular protein content, the SRB assay was used.³⁴ Cells were fixed with ice-cold 1% (v/v) acetic acid in methanol overnight at -20°C . Fixative was aspirated and plates were allowed to dry at 37°C before proceeding to the next step. SRB (0.5% (w/v) in 1% (v/v) acetic acid in dH₂O) was incubated in wells (37°C , 30 minutes). SRB was then aspirated, and unbound stain was removed by extensive washing using 1% acetic acid, prior to drying plates at 37°C . The bound protein stain was solubilised by shaking incubation with 10 mM Tris (pH 10; 15 min, RT). Absorbance was read on a microplate reader with a 544/15 nm filter.

TMRM assays

For analysis of the mitochondrial membrane potential, TMRM accumulation at mitochondria was visualised by fluorescence microscopy, as described previously.³⁵ HeLa cells were seeded in 35 mm glass-bottomed dishes and incubated until they reached approximately 70% confluency. They were then washed with HBSS and incubated in imaging buffer (HBSS supplemented with 10 mM D-glucose, 10 mM HEPES, 2 mM MgSO₄, 2 mM CaCl₂, 1.25 mM KH₂PO₄, pH 7.35) with 20 nM TMRM and 1 $\mu\text{g/ml}$ Hoechst 33342 for 30 min at 37°C . Cells were then washed with HBSS and incubated in imaging buffer with 20 nM TMRM. Cells were then imaged for 10 min, with TMRM retained in the buffer. For the AO sample, 1 μM antimycin A, and 5 μM oligomycin were added and cells were imaged for a further 10 min. Then, 10 μM CCCP was added, and cells were imaged for a further 10 min (for both control and +AO samples). Imaging was done using a Leica SP8 confocal microscope with LAS X software, at 37°C .

Statistical analysis

Statistical significance between groups was determined using unpaired Student's t-Test or one-way ANOVA with interaction if more than two groups were analysed. Following ANOVA, p values were adjusted for multiple comparisons through Tukey's post-hoc test and differences were considered significant at 5% level. Statistical analyses were performed using Graph Pad Prism version 9 (GraphPad Software, Inc., San Diego, CA, USA). Ns = $p > 0.05$, * = $p \leq 0.05$, ** = $p \leq 0.01$, *** = $p \leq 0.001$, **** = $p \leq 0.0001$.

Funding

This work was funded by the Wellcome Trust: to HIN and JSL through the Wellcome Trust Dynamic Molecular Cell Biology PhD programme

(083474) and IC by a Wellcome Investigator award (104632).

The funder had no role in study design, data collection and interpretation, or the decision to submit the work for publication. For the purpose of Open Access, the authors have applied a CC BY public copyright license to any Author Accepted Manuscript version arising from this submission.

Data and materials availability

All data are available in the main text or the [supplementary materials](#).

DATA AVAILABILITY

Data will be made available on request.

Acknowledgments

Thank you to Dr Natalie Niemi for the suggestion of 'MitoLuc'—good shout!

Author contribution

HIN, JSL, GCP and IC designed experiments; HIN and JSL conducted experiments; HIN and IC wrote the manuscript; HIN, GCP, JMH, and IC edited the manuscript; IC secured funding and led the project.

Declaration of Competing Interest

The authors declare that they have no known competing financial interests or personal relationships that could have appeared to influence the work reported in this paper.

Appendix A. Supplementary Data

Supplementary data to this article can be found online at <https://doi.org/10.1016/j.jmb.2023.168129>.

Received 8 December 2022;

Accepted 19 April 2023;

Available online 25 April 2023

Keywords:

mitochondria;
protein import;
in-cell assay;
split luciferase;
nanoluc;
mitoluc

† Current Address: Nanna Therapeutics, Merrifield Centre, Rosemary Lane, Cambridge CB1 3LQ, UK.

References

- Neupert, W., (1997). Protein import into mitochondria. *Annu. Rev. Biochem.* **66**, 863–917.
- Needs, H.I., Protasoni, M., Henley, J.M., Prudent, J., Collinson, I., Pereira, G.C., (2021). Interplay between Mitochondrial Protein Import and Respiratory Complexes Assembly in Neuronal Health and Degeneration. *Life-Basel*. **11**
- Sokol, A.M., Sztolsztener, M.E., Wasilewski, M., Heinz, E., Chacinska, A., (2014). Mitochondrial protein translocases for survival and wellbeing. *FEBS Lett.* **588**, 2484–2495.
- Devi, L., Prabhu, B.M., Galati, D.F., Avadhani, N.G., Anandatheerthavarada, H.K., (2006). Accumulation of amyloid precursor protein in the mitochondrial import channels of human Alzheimer's disease brain is associated with mitochondrial dysfunction. *J. Neurosci.* **26**, 9057–9068.
- Devi, L., Raghavendran, V., Prabhu, B.M., Avadhani, N.G., Anandatheerthavarada, H.K., (2008). Mitochondrial import and accumulation of alpha-synuclein impair complex I in human dopaminergic neuronal cultures and Parkinson disease brain. *J. Biol. Chem.* **283**, 9089–9100.
- Yano, H., Baranov, S.V., Baranova, O.V., Kim, J., Pan, Y. C., Yablonska, S., et al., (2014). Inhibition of mitochondrial protein import by mutant huntingtin. *Nat. Neurosci.* **17**, 822–831.
- Di Maio, R., Barrett, P.J., Hoffman, E.K., Barrett, C.W., Zharikov, A., Borah, A., et al., (2016). alpha-Synuclein binds to TOM20 and inhibits mitochondrial protein import in Parkinson's disease. *Sci. Transl. Med.* **8**, 14.
- Kang, P.J., Ostermann, J., Shilling, J., Neupert, W., Craig, E.A., Pfanner, N., (1990). Requirement for HSP70 in the mitochondrial matrix for translocation and folding of precursor proteins. *Nature* **348**, 137–143.
- Miyata, N., Steffen, J., Johnson, M.E., Fargue, S., Danpure, C.J., Koehler, C.M., (2014). Pharmacologic rescue of an enzyme-trafficking defect in primary hyperoxaluria 1. *PNAS* **111**, 14406–14411.
- Miyata, N., Tang, Z.Y., Conti, M.A., Johnson, M.E., Douglas, C.J., Hasson, S.A., et al., (2017). Adaptation of a Genetic Screen Reveals an Inhibitor for Mitochondrial Protein Import Component Tim44. *J. Biol. Chem.* **292**, 5429–5442.
- Dixon, A.S., Schwinn, M.K., Hall, M.P., Zimmerman, K., Otto, P., Lubben, T.H., et al., (2016). NanoLuc Complementation Reporter Optimized for Accurate Measurement of Protein Interactions in Cells. *ACS Chem. Biol.* **11**, 400–408.
- Pereira, G.C., Allen, W.J., Watkins, D.W., Buddrus, L., Noone, D., Liu, X., et al., (2019). A High-Resolution Luminescent Assay for Rapid and Continuous Monitoring of Protein Translocation across Biological Membranes. *J. Mol. Biol.* **431**, 1689–1699.
- Smoyer, C.J., Katta, S.S., Gardner, J.M., Stoltz, L., McCroskey, S., Bradford, W.D., et al., (2016). Analysis of membrane proteins localizing to the inner nuclear envelope in living cells. *J. Cell Biol.* **215**, 575–590.
- Wehrman, T.S., Casipit, C.L., Gewertz, N.M., Blau, H.M., (2005). Enzymatic detection of protein translocation. *Nat. Methods* **2**, 521–527.
- Krayl, M., Guiard, B., Paal, K., Voos, W., (2006). Fluorescence-mediated analysis of mitochondrial preprotein import in vitro. *Anal. Biochem.* **355**, 81–89.
- Hall, M.P., Unch, J., Binkowski, B.F., Valley, M.P., Butler, B.L., Wood, M.G., et al., (2012). Engineered Luciferase Reporter from a Deep Sea Shrimp Utilizing a Novel Imidazopyrazinone Substrate. *ACS Chem. Biol.* **7**, 1848–1857.
- England, C.G., Ehlerding, E.B., Cai, W.B., (2016). NanoLuc: A Small Luciferase Is Brightening Up the Field of Bioluminescence. *Bioconjug. Chem.* **27**, 1175–1187.
- Ford, H.C., Allen, W.J., Pereira, G.C., Liu, X., Dillingham, M.S., Collinson, I., (2022). Towards a molecular mechanism underlying mitochondrial protein import through the TOM and TIM23 complexes. *Elife* **11**
- Allen, W.J., Watkins, D.W., Dillingham, M.S., Collinson, I., (2020). Refined measurement of SecA-driven protein secretion reveals that translocation is indirectly coupled to ATP turnover. *PNAS* **117**, 31808–318016.
- Allen, W.J., Corey, R.A., Watkins, D.W., Oliveira, A.S.F., Hards, K., Cook, G.M., et al., (2022). Rate-limiting transport of positively charged arginine residues through the Sec-machinery is integral to the mechanism of protein secretion. *Elife* **11**, 23.
- Daniels, R.W., Rossano, A.J., Macleod, G.T., Ganetzky, B., (2014). Expression of Multiple Transgenes from a Single Construct Using Viral 2A Peptides in Drosophila. *PLoS One* **9**, 10.
- Shcherbo, D., Shemiakina, I.I., Ryabova, A.V., Luker, K.E., Schmidt, B.T., Souslova, E.A., et al., (2010). Near-infrared fluorescent proteins. *Nat. Methods* **7** 827-U1520.
- Kacprzyk-Stokowiec, A., Kulma, M., Traczyk, G., Kwiatkowska, K., Sobota, A., Dadlez, M., (2014). Crucial Role of Perfringolysin O D1 Domain in Orchestrating Structural Transitions Leading to Membrane-perforating Pores A Hydrogen-Deuterium Exchange Study. *J. Biol. Chem.* **289**, 28738–28752.
- Divakaruni, A.S., Wiley, S.E., Rogers, G.W., Andreyev, A. Y., Petrosyan, S., Loviscach, M., et al., (2013). Thiazolidinediones are acute, specific inhibitors of the mitochondrial pyruvate carrier. *PNAS* **110**, 5422–5427.
- Rossjohn, J., Polekhina, G., Feil, S.C., Morton, C.J., Tweten, R.K., Parker, M.W., (2007). Structures of perfringolysin O suggest a pathway for activation of cholesterol-dependent cytolysins. *J. Mol. Biol.* **367**, 1227–1236.
- Ramachandran, R., Heuck, A.P., Tweten, R.K., Johnson, A.E., (2002). Structural insights into the membrane-anchoring mechanism of a cholesterol-dependent cytolysin. *Nat. Struct. Biol.* **9**, 823–827.
- Dixon, A.S., Encell, L., Hall, M., Wood, K., Wood, M., Schwinn, M., et al., (2017). Activation of bioluminescence by structural complementation. Promega Corporation, USA.
- Williamson, D.S., Borgognoni, J., Clay, A., Daniels, Z., Dokurno, P., Drysdale, M.J., et al., (2009). Novel Adenosine-Derived Inhibitors of 70 kDa Heat Shock Protein, Discovered Through Structure-Based Design. *J. Med. Chem.* **52**, 1510–1513.
- ModicaNapolitano, J.S., Koya, K., Weisberg, E., Brunelli, B.T., Li, Y., Chen, L.B., (1996). Selective damage to carcinoma mitochondria by the rhodocyanine MKT-077. *Cancer Res.* **56**, 544–550.
- Wisén, S., Bertelsen, E.B., Thompson, A.D., Patury, S., Ung, P., Chang, L., et al., (2010). Binding of a Small Molecule at a Protein-Protein Interface Regulates the Chaperone Activity of Hsp70-Hsp40. *ACS Chem. Biol.* **5**, 611–622.

31. Dabir, D.V., Hasson, S.A., Setoguchi, K., Johnson, M.E., Wongkongkathep, P., Douglas, C.J., et al., (2013). A Small Molecule Inhibitor of Redox-Regulated Protein Translocation into Mitochondria. *Dev. Cell* **25**, 81–92.
32. Stojanovski, D., Muller, J.M., Milenkovic, D., Guiard, B., Pfanner, N., Chacinska, A., (2008). The MIA system for protein import into the mitochondrial intermembrane space. *BBA-Mol. Cell. Res.* **1783**, 610–617.
33. Pickrell, A.M., Youle, R.J., (2015). The Roles of PINK1, Parkin, and Mitochondrial Fidelity in Parkinson's Disease. *Neuron* **85**, 257–273.
34. Vichai, V., Kirtikara, K., (2006). Sulforhodamine B colorimetric assay for cytotoxicity screening. *Nat. Protoc.* **1**, 1112–1116.
35. Creed, S., McKenzie, M., (2019). Measurement of Mitochondrial Membrane Potential with the Fluorescent Dye Tetramethylrhodamine Methyl Ester (TMRM). In: Haznadar, M. (Ed.), *Cancer Metabolism: Methods and Protocols*. Springer, New York, New York, NY, pp. 69–76.